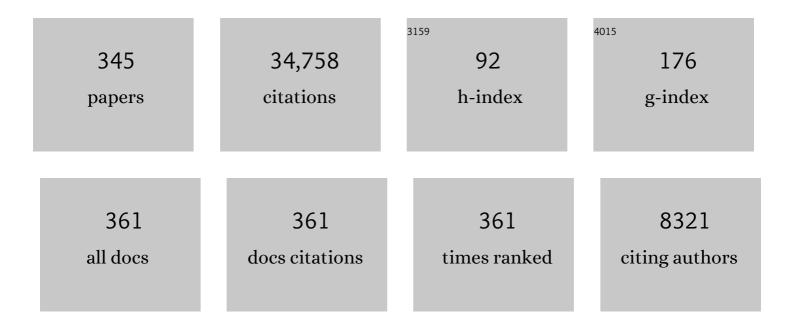
List of Publications by Year in descending order

Source: https://exaly.com/author-pdf/7755602/publications.pdf Version: 2024-02-01



#	Article	IF	CITATIONS
1	Archean blocks and their boundaries in the North China Craton: lithological, geochemical, structural and P–T path constraints and tectonic evolution. Precambrian Research, 2001, 107, 45-73.	2.7	1,657
2	Review of global 2.1–1.8 Ga orogens: implications for a pre-Rodinia supercontinent. Earth-Science Reviews, 2002, 59, 125-162.	9.1	1,388
3	Precambrian geology of China. Precambrian Research, 2012, 222-223, 13-54.	2.7	1,241
4	Detrital zircon record and tectonic setting. Geology, 2012, 40, 875-878.	4.4	1,038
5	Amalgamation of the North China Craton: Key issues and discussion. Precambrian Research, 2012, 222-223, 55-76.	2.7	806
6	Accretionary orogens through Earth history. Geological Society Special Publication, 2009, 318, 1-36.	1.3	719
7	A Change in the Geodynamics of Continental Growth 3 Billion Years Ago. Science, 2012, 335, 1334-1336.	12.6	707
8	The generation and evolution of the continental crust. Journal of the Geological Society, 2010, 167, 229-248.	2.1	650
9	Terra Australis Orogen: Rodinia breakup and development of the Pacific and Iapetus margins of Gondwana during the Neoproterozoic and Paleozoic. Earth-Science Reviews, 2005, 69, 249-279.	9.1	635
10	Metamorphism of basement rocks in the Central Zone of the North China Craton: implications for Paleoproterozoic tectonic evolution. Precambrian Research, 2000, 103, 55-88.	2.7	566
11	Linking accretionary orogenesis with supercontinent assembly. Earth-Science Reviews, 2007, 82, 217-256.	9.1	562
12	Thermal Evolution of Archean Basement Rocks from the Eastern Part of the North China Craton and Its Bearing on Tectonic Setting. International Geology Review, 1998, 40, 706-721.	2.1	557
13	Locating South China in Rodinia and Gondwana: A fragment of greater India lithosphere?. Geology, 2013, 41, 903-906.	4.4	529
14	The continental record and the generation of continental crust. Bulletin of the Geological Society of America, 2013, 125, 14-32.	3.3	484
15	Assembly of the Lhasa and Qiangtang terranes in central Tibet by divergent double subduction. Lithos, 2016, 245, 7-17.	1.4	432
16	High-Pressure Granulites (Retrograded Eclogites) from the Hengshan Complex, North China Craton: Petrology and Tectonic Implications. Journal of Petrology, 2001, 42, 1141-1170.	2.8	417
17	Early Palaeozoic orogenesis along the Indian margin of Gondwana: Tectonic response to Gondwana assembly. Earth and Planetary Science Letters, 2007, 255, 70-84.	4.4	417
18	Single zircon grains record two Paleoproterozoic collisional events in the North China Craton. Precambrian Research, 2010, 177, 266-276.	2.7	414

#	Article	IF	CITATIONS
19	SHRIMP U-Pb zircon ages of the Fuping Complex: Implications for Late Archean to Paleoproterozoic accretion and assembly of the North China Craton. Numerische Mathematik, 2002, 302, 191-226.	1.4	400
20	Opening lapetus: Constraints from the Laurentian margin in Newfoundland. Bulletin of the Geological Society of America, 2001, 113, 443-453.	3.3	369
21	Reconstructing South China in Phanerozoic and Precambrian supercontinents. Earth-Science Reviews, 2018, 186, 173-194.	9.1	364
22	Tectonic setting of the South China Block in the early Paleozoic: Resolving intracontinental and ocean closure models from detrital zircon U-Pb geochronology. Tectonics, 2010, 29, n/a-n/a.	2.8	345
23	When Continents Formed. Science, 2011, 331, 154-155.	12.6	324
24	A Matter of Preservation. Science, 2009, 323, 49-50.	12.6	319
25	Magmatic record of India-Asia collision. Scientific Reports, 2015, 5, 14289.	3.3	316
26	Linking collisional and accretionary orogens during Rodinia assembly and breakup: Implications for models of supercontinent cycles. Earth and Planetary Science Letters, 2016, 449, 118-126.	4.4	316
27	Sedimentary basin and detrital zircon record along East Laurentia and Baltica during assembly and breakup of Rodinia. Journal of the Geological Society, 2007, 164, 257-275.	2.1	292
28	Tectonothermal history of the basement rocks in the western zone of the North China Craton and its tectonic implications. Tectonophysics, 1999, 310, 37-53.	2.2	290
29	Granitoid evolution in the Late Archean Wutai Complex, North China Craton. Journal of Asian Earth Sciences, 2005, 24, 597-613.	2.3	286
30	Assembling Australia: Proterozoic building of a continent. Precambrian Research, 2008, 166, 1-35.	2.7	284
31	Provenance record of a rift basin: U/Pb ages of detrital zircons from the Perth Basin, Western Australia. Sedimentary Geology, 2000, 134, 209-234.	2.1	270
32	Early Paleozoic and Early Mesozoic intraplate tectonic and magmatic events in the Cathaysia Block, South China. Tectonics, 2015, 34, 1600-1621.	2.8	262
33	Precambrian plate tectonics: Criteria and evidence. GSA Today, 2006, 16, 4.	2.0	249
34	Tectonics and crustal evolution. GSA Today, 2016, 26, 4-11.	2.0	246
35	Thermal evolution of two textural types of mafic granulites in the North China craton: evidence for both mantle plume and collisional tectonics. Geological Magazine, 1999, 136, 223-240.	1.5	236
36	Closure of the East Paleotethyan Ocean and amalgamation of the Eastern Cimmerian and Southeast Asia continental fragments. Earth-Science Reviews, 2018, 186, 195-230.	9.1	231

#	Article	IF	CITATIONS
37	Geological archive of the onset of plate tectonics. Philosophical Transactions Series A, Mathematical, Physical, and Engineering Sciences, 2018, 376, 20170405.	3.4	227
38	Geochronological, geochemical and Nd–Hf–Os isotopic fingerprinting of an early Neoproterozoic arc–back-arc system in South China and its accretionary assembly along the margin of Rodinia. Precambrian Research, 2013, 231, 343-371.	2.7	218
39	Linking source and sedimentary basin: Detrital zircon record of sediment flux along a modern river system and implications for provenance studies. Earth and Planetary Science Letters, 2003, 210, 259-268.	4.4	202
40	Neoproterozoic orogeny along the margin of Rodinia: Valhalla orogen, North Atlantic. Geology, 2010, 38, 99-102.	4.4	199
41	Petrology and P-T path of the Fuping mafic granulites: implications for tectonic evolution of the central zone of the North China craton. Journal of Metamorphic Geology, 2000, 18, 375-391.	3.4	195
42	Sr–Nd–Pb isotopic constraints on multiple mantle domains for Mesozoic mafic rocks beneath the South China Block hinterland. Lithos, 2008, 106, 297-308.	1.4	189
43	Assembling and reactivating the Proterozoic Capricorn Orogen: lithotectonic elements, orogenies, and significance. Precambrian Research, 2004, 128, 201-218.	2.7	186
44	Jiangnan Orogen, South China: A ~970–820â€ <sup>−</sup> Ma Rodinia margin accretionary belt. Earth-Science Reviews, 2019, 196, 102872.	9.1	186
45	Earth's middle age. Geology, 2014, 42, 503-506.	4.4	182
46	Earth's Continental Lithosphere Through Time. Annual Review of Earth and Planetary Sciences, 2017, 45, 169-198.	11.0	182
47	Raising the Cangdese Mountains in southern Tibet. Journal of Geophysical Research: Solid Earth, 2017, 122, 214-223.	3.4	178
48	Large Igneous Province and magmatic arc sourced Permian–Triassic volcanogenic sediments in China. Sedimentary Geology, 2012, 261-262, 120-131.	2.1	174
49	Paleogeographic development of the east Laurentian margin: Constraints from U-Pb dating of detrital zircons in the Newfoundland Appalachians. Bulletin of the Geological Society of America, 2001, 113, 1234-1246.	3.3	172
50	Geochemical, Sr-Nd-Pb, and Zircon Hf-O Isotopic Compositions of Eocene-Oligocene Shoshonitic and Potassic Adakite-like Felsic Intrusions in Western Yunnan, SW China: Petrogenesis and Tectonic Implications. Journal of Petrology, 2013, 54, 1309-1348.	2.8	170
51	Petrology and P–T history of the Wutai amphibolites: implications for tectonic evolution of the Wutai Complex, China. Precambrian Research, 1999, 93, 181-199.	2.7	168
52	Tarim and North China cratons linked to northern Gondwana through switching accretionary tectonics and collisional orogenesis. Geology, 2016, 44, 95-98.	4.4	167
53	Geology and timing of mineralization at the Cangshang gold deposit, north-western Jiaodong Peninsula, China. Mineralium Deposita, 2003, 38, 141-153.	4.1	158
54	Source of the Dalradian Supergroup constrained by U–Pb dating of detrital zircon and implications for the East Laurentian margin. Journal of the Geological Society, 2003, 160, 231-246.	2.1	152

#	Article	IF	CITATIONS
55	Triassic collision in the Paleo-Tethys Ocean constrained by volcanic activity in SW China. Lithos, 2012, 144-145, 145-160.	1.4	145
56	Petrogenesis of early Paleozoic peraluminous granite in the Sibumasu Block of SW Yunnan and diachronous accretionary orogenesis along the northern margin of Gondwana. Lithos, 2013, 182-183, 67-85.	1.4	144
57	Intracontinental Eocene-Oligocene Porphyry Cu Mineral Systems of Yunnan, Western Yangtze Craton, China: Compositional Characteristics, Sources, and Implications for Continental Collision Metallogeny. Economic Geology, 2013, 108, 1541-1576.	3.8	144
58	Rates of generation and growth of the continental crust. Geoscience Frontiers, 2019, 10, 165-173.	8.4	143
59	Paleoproterozoic magmatic and metamorphic events link Yangtze to northwest Laurentia in the Nuna supercontinent. Earth and Planetary Science Letters, 2016, 433, 269-279.	4.4	138
60	Continental growth and the crustal record. Tectonophysics, 2013, 609, 651-660.	2.2	135
61	Contrasting modes of supercontinent formation and the conundrum of Pangea. Gondwana Research, 2009, 15, 408-420.	6.0	133
62	Generation of Early Indosinian enriched mantle-derived granitoid pluton in the Sanjiang Orogen (SW) Tj ETQq0 (	0 0 <sub>[g</sub> BT /C	)verlock 10 Tf
63	Discordance of the U–Pb system in detrital zircons: Implication for provenance studies of sedimentary rocks. Sedimentary Geology, 2005, 182, 143-162.	2.1	130
64	Composition of back-arc basin volcanics, Valu Fa Ridge, Lau Basin: Evidence for a slab-derived component in their mantle source. Journal of Volcanology and Geothermal Research, 1987, 32, 209-222.	2.1	129
65	Detrital record of Indosinian mountain building in SW China: Provenance of the Middle Triassic turbidites in the Youjiang Basin. Tectonophysics, 2012, 574-575, 105-117.	2.2	128
66	Orogenesis without collision: Stabilizing the Terra Australis accretionary orogen, eastern Australia. Bulletin of the Geological Society of America, 2011, 123, 2240-2255.	3.3	125
67	Laurentia-Baltica-Amazonia relations during Rodinia assembly. Precambrian Research, 2017, 292, 386-397.	2.7	122
68	Zircon SHRIMP U–Pb geochronology of potassic felsic intrusions in western Yunnan, SW China: Constraints on the relationship of magmatism to the Jinsha suture. Gondwana Research, 2012, 22, 737-747.	6.0	121
69	U/Pb dating of detrital zircons: Implications for the provenance record of Gondwana margin terranes. Bulletin of the Geological Society of America, 1999, 111, 1107-1119.	3.3	119
70	Indosinian highâ€strain deformation for the Yunkaidashan tectonic belt, south China: Kinematics and <sup>40</sup> Ar/ <sup>39</sup> Ar geochronological constraints. Tectonics, 2007, 26, .	2.8	119

71	Linking south China to northern Australia and India on the margin of Gondwana: Constraints from detrital zircon U-Pb and Hf isotopes in Cambrian strata. Tectonics, 2013, 32, 1547-1558.	2.8	117
72	Generation and preservation of continental crust in the Grenville Orogeny. Geoscience Frontiers, 2015, 6, 357-372.	8.4	117

#	Article	IF	CITATIONS
73	Deconstructing South China and consequences for reconstructing Nuna and Rodinia. Earth-Science Reviews, 2020, 204, 103169.	9.1	115
74	Laurentian provenance and an intracratonic tectonic setting for the Moine Supergroup, Scotland, constrained by detrital zircons from the Loch Eil and Glen Urquhart successions. Journal of the Geological Society, 2004, 161, 861-874.	2.1	114
75	Record of Tethyan ocean closure and Indosinian collision along the Ailaoshan suture zone (SW) Tj ETQq1 1 0.78	4314 rgBT 6.0	Överlock 10
76	Petrogenesis of Early to Middle Jurassic granitoid rocks from the Gangdese belt, Southern Tibet: Implications for early history of the Neo-Tethys. Lithos, 2013, 179, 320-333.	1.4	112
77	Late Permian-Triassic magmatic evolution in the Jinshajiang orogenic belt, SW China and implications for orogenic processes following closure of the Paleo-Tethys. Numerische Mathematik, 2013, 313, 81-112.	1.4	112
78	Proterozoic onset of crustal reworking and collisional tectonics: Reappraisal of the zircon oxygen isotope record. Geology, 2014, 42, 451-454.	4.4	110
79	Gangdese magmatism in southern Tibet and India–Asia convergence since 120 Ma. Geological Society Special Publication, 2019, 483, 583-604.	1.3	110
80	An Andean-type retro-arc foreland system beneath northwest South China revealed by SINOPROBE profiling. Earth and Planetary Science Letters, 2018, 490, 170-179.	4.4	109
81	Was Baltica right-way-up or upside-down in the Neoproterozoic?. Journal of the Geological Society, 2006, 163, 753-759.	2.1	107
82	Metallogeny of accretionary orogens — The connection between lithospheric processes and metal endowment. Ore Geology Reviews, 2009, 36, 282-292.	2.7	106
83	Subalkaline andesite from Valu Fa Ridge, a back-arc spreading center in southern Lau Basin: petrogenesis, comparative chemistry, and tectonic implications. Chemical Geology, 1991, 91, 227-256.	3.3	103
84	Mercury anomalies across the end Permian mass extinction in South China from shallow and deep water depositional environments. Earth and Planetary Science Letters, 2018, 496, 159-167.	4.4	103
85	Contrasting rift and subductionâ€related plagiogranites in the Jinshajiang ophiolitic mélange, southwest China, and implications for the Paleoâ€Tethys. Tectonics, 2012, 31, .	2.8	102
86	Late Neoarchean subduction-related crustal growth in the Northern Liaoning region of the North China Craton: Evidence from â°¼2.55 to 2.50 Ga granitoid gneisses. Precambrian Research, 2016, 281, 200-223.	2.7	102
87	Modal composition and detrital clinopyroxene geochemistry of lithic sandstones from the New England Fold Belt (east Australia): A Paleozoic forearc terrane. Bulletin of the Geological Society of America, 1983, 94, 1199.	3.3	101
88	Generation and obduction of ophiolites: Constraints from the Bay of Islands Complex, western Newfoundland. Tectonics, 1992, 11, 884-897.	2.8	100
89	Short episodes of crust generation during protracted accretionary processes: Evidence from Central Asian Orogenic Belt, NW China. Earth and Planetary Science Letters, 2017, 464, 142-154.	4.4	98
90	Closure of the Clymene Ocean and formation of West Gondwana in the Cambrian: Evidence from the Sierras Australes of the southernmost Rio de la Plata craton, Argentina. Gondwana Research, 2012, 21, 394-405.	6.0	95

#	Article	IF	CITATIONS
91	Neoproterozoic subduction along the Ailaoshan zone, South China: Geochronological and geochemical evidence from amphibolite. Precambrian Research, 2014, 245, 13-28.	2.7	95
92	The Evolution of the Continental Crust and the Onset of Plate Tectonics. Frontiers in Earth Science, 2020, 8, .	1.8	95
93	Detrital zircon record of continental collision: Assembly of the Qilian Orogen, China. Sedimentary Geology, 2010, 230, 35-45.	2.1	94
94	Late Neoproterozoic and Early Cambrian palaeogeography: models and problems. Geological Society Special Publication, 2008, 294, 9-31.	1.3	92
95	Intraplate orogenesis in response to Gondwana assembly: Kwangsian Orogeny, South China. Numerische Mathematik, 2016, 316, 329-362.	1.4	91
96	Unraveling the New England orocline, east Gondwana accretionary margin. Tectonics, 2011, 30, .	2.8	90
97	Lowâ€Î´ <sup>18</sup> 0 Rhyolites From the Malani Igneous Suite: A Positive Test for South China and NW India Linkage in Rodinia. Geophysical Research Letters, 2017, 44, 10,298.	4.0	90
98	U–Pb detrital zircon ages and Sm–Nd isotopic features in low-grade metasedimentary rocks of the Famatina belt: implications for late Neoproterozoic–early Palaeozoic evolution of the proto-Andean margin of Gondwana. Journal of the Geological Society, 2009, 166, 303-319.	2.1	89
99	Provenance record of Laurentian passive-margin strata in the northern Caledonides: Implications for paleodrainage and paleogeography. Bulletin of the Geological Society of America, 2007, 119, 993-1003.	3.3	87
100	Timing of peak metamorphism and deformation along the Appalachian margin of Laurentia in Newfoundland: Silurian, not Ordovician. Geology, 1994, 22, 399.	4.4	86
101	Not all supercontinents are created equal: Gondwana-Rodinia case study. Geology, 2013, 41, 795-798.	4.4	81
102	Continental growth seen through the sedimentary record. Sedimentary Geology, 2017, 357, 16-32.	2.1	81
103	Early Paleozoic orogenesis along Gondwana's northern margin constrained by provenance data from South China. Tectonophysics, 2014, 636, 40-51.	2.2	79
104	Delineating and characterizing the boundary of the Cathaysia Block and the Jiangnan orogenic belt in South China. Precambrian Research, 2016, 275, 265-277.	2.7	79
105	SHRIMP U-Pb zircon dating of granites and gneisses in the taihangshan-wutaishan area: Implications for the timing of crustal growth in the North China Craton. Science Bulletin, 1998, 43, 144-144.	1.7	78
106	The tectonic and metallogenic framework of Myanmar: A Tethyan mineral system. Ore Geology Reviews, 2016, 79, 26-45.	2.7	78
107	Zircon U–Pb age and Hf isotope evidence for an Eoarchaean crustal remnant and episodic crustal reworking in response to supercontinent cycles in NW India. Journal of the Geological Society, 2017, 174, 759-772.	2.1	78
108	Building Southeast China in the late Mesozoic: Insights from alternating episodes of shortening and extension along the Lianhuashan fault zone. Earth-Science Reviews, 2020, 201, 103056.	9.1	78

#	Article	IF	CITATIONS
109	Structural Relations in the Subduction Complex of the Paleozoic New England Fold Belt, Eastern Australia. Journal of Geology, 1982, 90, 381-392.	1.4	77
110	Global continental weathering trends across the Early Permian glacial to postglacial transition: Correlating high- and low-paleolatitude sedimentary records. Geology, 2014, 42, 835-838.	4.4	76
111	Geochronological constraints on the age of a Permo–Triassic impact event: U–Pb and 40Ar/39Ar results for the 40km Araguainha structure of central Brazil. Geochimica Et Cosmochimica Acta, 2012, 86, 214-227.	3.9	74
112	One or Two Early Cretaceous Arc Systems in the Lhasa Terrane, Southern Tibet. Journal of Geophysical Research: Solid Earth, 2018, 123, 3391-3413.	3.4	74
113	When crust comes of age: on the chemical evolution of Archaean, felsic continental crust by crustal drip tectonics. Philosophical Transactions Series A, Mathematical, Physical, and Engineering Sciences, 2018, 376, 20180103.	3.4	74
114	Determining Precambrian crustal evolution in China: a case-study from Wutaishan, Shanxi Province, demonstrating the application of precise SHRIMP U-Pb geochronology. Geological Society Special Publication, 2004, 226, 5-25.	1.3	73
115	Evolution of the Appalachian Laurentian margin: Lithoprobe results in western Newfoundland. Canadian Journal of Earth Sciences, 1998, 35, 1271-1287.	1.3	72
116	Terminal suturing of Gondwana along the southern margin of South China Craton: Evidence from detrital zircon U-Pb ages and Hf isotopes in Cambrian and Ordovician strata, Hainan Island. Tectonics, 2014, 33, 2490-2504.	2.8	72
117	Clobal mercury cycle during the end-Permian mass extinction and subsequent Early Triassic recovery. Earth and Planetary Science Letters, 2019, 513, 144-155.	4.4	72
118	Late Paleozoic to Early Mesozoic provenance record of Paleoâ€Pacific subduction beneath South China. Tectonics, 2015, 34, 986-1008.	2.8	70
119	Geochronological, elemental and Sr-Nd-Hf-O isotopic constraints on the petrogenesis of the Triassic post-collisional granitic rocks in NW Thailand and its Paleotethyan implications. Lithos, 2016, 266-267, 264-286.	1.4	70
120	Provenance record of a foreland basin: Detrital zircon U–Pb ages from Devonian strata in the North Qilian Orogenic Belt, China. Tectonophysics, 2010, 495, 337-347.	2.2	69
121	Neoproterozoic crustal growth of the Southern Yangtze Block: Geochemical and zircon U–Pb geochronological and Lu-Hf isotopic evidence of Neoproterozoic diorite from the Ailaoshan zone. Precambrian Research, 2015, 266, 137-149.	2.7	68
122	Gondwana's interlinked peripheral orogens. Earth and Planetary Science Letters, 2021, 568, 117057.	4.4	68
123	From sediments to their source rocks: Hf and Nd isotopes in recent river sediments. Geology, 2011, 39, 407-410.	4.4	65
124	Continental crustal volume, thickness and area, and their geodynamic implications. Gondwana Research, 2019, 66, 116-125.	6.0	64
125	Structural styles in the Perth Basin associated with the Mesozoic break-up of Greater India and Australia. Tectonophysics, 2000, 317, 55-72.	2.2	62
126	Permianâ€Jurassic strata at Productus Creek, Southland, New Zealand: Implications for terrane dynamics of the eastern Gondwanaland margin. New Zealand Journal of Geology, and Geophysics, 1999, 42, 255-278.	1.8	61

#	Article	IF	CITATIONS
127	Detrital zircon geochronology of the Grenville/Llano foreland and basal Sauk Sequence in west Texas, USA. Bulletin of the Geological Society of America, 2014, 126, 1117-1128.	3.3	61
128	Voluminous silicic eruptions during late Permian Emeishan igneous province and link to climate cooling. Earth and Planetary Science Letters, 2015, 432, 166-175.	4.4	60
129	Mantle influx compensates crustal thinning beneath the Cathaysia Block, South China: Evidence from SINOPROBE reflection profiling. Earth and Planetary Science Letters, 2020, 544, 116360.	4.4	60
130	Silurian collisional suturing onto the southern margin of the North China craton: Detrital zircon geochronology constraints from the Qilian Orogen. Sedimentary Geology, 2009, 220, 95-104.	2.1	59
131	Early Wuchiapingian cooling linked to Emeishan basaltic weathering?. Earth and Planetary Science Letters, 2018, 492, 102-111.	4.4	58
132	No collision between Eastern and Western Gondwana at their northern extent. Geology, 2019, 47, 308-312.	4.4	58
133	Geochemistry of Paleoproterozoic (â^1⁄41770Ma) mafic dikes from the Trans-North China Orogen and tectonic implications. Journal of Asian Earth Sciences, 2008, 33, 61-77.	2.3	57
134	Temporal relations between mineral deposits and global tectonic cycles. Geological Society Special Publication, 2015, 393, 9-21.	1.3	56
135	Extensive crustal extraction in Earth's early history inferred from molybdenum isotopes. Nature Geoscience, 2019, 12, 946-951.	12.9	55
136	Provenance of Late Permian volcanic ash beds in South China: Implications for the age of Emeishan volcanism and its linkage to climate cooling. Lithos, 2018, 314-315, 293-306.	1.4	54
137	U-Pb geochronology and geochemistry of the Dashibao Basalts in the Songpan-Ganzi Terrane, SW China, with implications for the age of Emeishan volcanism. Numerische Mathematik, 2010, 310, 1054-1080.	1.4	53
138	Neoproterozoic to early Paleozoic extensional and compressional history of East Laurentian margin sequences: The Moine Supergroup, Scottish Caledonides. Bulletin of the Geological Society of America, 2015, 127, 349-371.	3.3	53
139	Eocene magmatic processes and crustal thickening in southern Tibet: Insights from strongly fractionated ca. 43Ma granites in the western Gangdese Batholith. Lithos, 2015, 239, 128-141.	1.4	52
140	Evolving passive- and active-margin tectonics of the Paleoproterozoic Aravalli Basin, NW India. Bulletin of the Geological Society of America, 2019, 131, 426-443.	3.3	52
141	Fragmentation of South China from greater India during the Rodinia-Gondwana transition. Geology, 2021, 49, 228-232.	4.4	52
142	Anticlockwise P-T evolution at â^1⁄4280Ma recorded from ultrahigh-temperature metapelitic granulite in the Chinese Altai orogenic belt, a possible link with the Tarim mantle plume?. Journal of Asian Earth Sciences, 2014, 94, 1-11.	2.3	51
143	Silicic ash beds bracket Emeishan Large Igneous province to < 1 m.y. at ~ 260 Ma. Lithos, 2016, 264, 17-27.	1.4	51
144	Reconstructing Early Permian tropical climates from chemical weathering indices. Bulletin of the Geological Society of America, 2016, 128, 739-751.	3.3	51

#	Article	IF	CITATIONS
145	Cyclic formation and stabilization of Archean lithosphere by accretionary orogenesis: Constraints from TTG and potassic granitoids, North China Craton. Tectonics, 2017, 36, 1724-1742.	2.8	51
146	The development of the SW Pacific Margin of Gondwana: Correlations between the Rangitata and New England Orogens. Tectonics, 1984, 3, 539-553.	2.8	50
147	Provenance record of the Jack Hills metasedimentary belt: Source of the Earth's oldest zircons. Precambrian Research, 2005, 138, 235-254.	2.7	50
148	The South American ancestry of the North Patagonian Massif: geochronological evidence for an autochthonous origin?. Terra Nova, 2013, 25, 337-342.	2.1	50
149	Peel-back controlled lithospheric convergence explains the secular transitions in Archean metamorphism and magmatism. Earth and Planetary Science Letters, 2020, 538, 116224.	4.4	49
150	Thermo-mechanical controls of flat subduction: Insights from numerical modeling. Gondwana Research, 2016, 40, 170-183.	6.0	48
151	Two-stage terrane assembly in Western Gondwana: Insights from structural geology and geophysical data of central Borborema Province, NE Brazil. Journal of Structural Geology, 2017, 103, 167-184.	2.3	46
152	Rates of generation and destruction of the continental crust: implications for continental growth. Philosophical Transactions Series A, Mathematical, Physical, and Engineering Sciences, 2018, 376, 20170403.	3.4	46
153	Highly Refractory Peridotites on Macquarie Island and the Case for Anciently Depleted Domains in the Earth's Mantle. Journal of Petrology, 2010, 51, 469-493.	2.8	45
154	Detrital records for Upper Permian-Lower Triassic succession in the Shiwandashan Basin, South China and implication for Permo-Triassic (Indosinian) orogeny. Journal of Asian Earth Sciences, 2015, 98, 152-166.	2.3	45
155	Enhanced continental weathering and large igneous province induced climate warming at the Permo-Carboniferous transition. Earth and Planetary Science Letters, 2020, 534, 116074.	4.4	45
156	Crustal rejuvenation stabilised Earth's first cratons. Nature Communications, 2021, 12, 3535.	12.8	45
157	Drivers for late Paleozoic to early Mesozoic orogenesis in South China: Constraints from the sedimentary record. Tectonophysics, 2014, 618, 107-120.	2.2	44
158	Reconciling thermal regimes and tectonics of the early Earth. Geology, 2019, 47, 923-927.	4.4	44
159	Geological development of eastern Humber and western Dunnage zones: Corner Brook–Glover Island region, Newfoundland. Canadian Journal of Earth Sciences, 1996, 33, 182-198.	1.3	43
160	Permian fragmentation, accretion and subsequent translation of a low-latitude Tethyan seamount to the high-latitude east Gondwana margin: evidence from detrital zircon age data. Geological Magazine, 2002, 139, 131-144.	1.5	43
161	High-T, low-P metamorphism in the Palaeoproterozoic Halls Creek Orogen, northern Australia: the middle crustal response to a mantle-related transient thermal pulse. Journal of Metamorphic Geology, 2002, 20, 217-237.	3.4	43
162	Neoarchean crustal growth and Paleoproterozoic reworking in the Borborema Province, NE Brazil: Insights from geochemical and isotopic data of TTG and metagranitic rocks of the Alto MoxotÅ <sup>3</sup> Terrane. Journal of South American Earth Sciences, 2017, 79, 342-363.	1.4	43

#	Article	IF	CITATIONS
163	Quantifying rates of dome-and-keel formation in the Barberton granitoid-greenstone belt, South Africa. Precambrian Research, 2010, 177, 199-211.	2.7	42
164	Intermontane basins and bimodal volcanism at the onset of the Sveconorwegian Orogeny, southern Norway. Precambrian Research, 2014, 252, 107-118.	2.7	42
165	An Early Neoproterozoic Accretionary Prism Ophiolitic Mélange from the Western Jiangnan Orogenic Belt, South China. Journal of Geology, 2016, 124, 587-601.	1.4	42
166	Neoarchean and Paleoproterozoic K-rich granites in the Phan Si Pan Complex, north Vietnam: Constraints on the early crustal evolution of the Yangtze Block. Precambrian Research, 2019, 332, 105395.	2.7	42
167	Earth Matters: A tempo to our planet's evolution. Geology, 2020, 48, 525-526.	4.4	42
168	Detrital zircon provenance of Upper Ordovician and Silurian strata in the northeastern Yangtze Block: Response to orogenesis in South China. Sedimentary Geology, 2012, 267-268, 63-72.	2.1	41
169	Eocene supra-subduction zone mafic magmatism in the Sibumasu Block of SW Yunnan: Implications for Neotethyan subduction and India–Asia collision. Lithos, 2014, 206-207, 384-399.	1.4	41
170	Late Neoarchean crust-mantle geodynamics: Evidence from Pingquan Complex of the Northern Hebei Province, North China Craton. Precambrian Research, 2017, 303, 470-493.	2.7	40
171	Origin of Permian OIB-like basalts in NW Thailand and implication on the Paleotethyan Ocean. Lithos, 2017, 274-275, 93-105.	1.4	40
172	Early Paleozoic accretionary orogenesis along northern margin of Gondwana constrained by high-Mg metaigneous rocks, SW Yunnan. International Journal of Earth Sciences, 2017, 106, 1469-1486.	1.8	39
173	Lithosphere differentiation in the early Earth controls Archean tectonics. Earth and Planetary Science Letters, 2019, 525, 115755.	4.4	38
174	Implication of Mesoproterozoic (â^¼1.4†Ga) magmatism within microcontinents along the southern Central Asian Orogenic Belt. Precambrian Research, 2019, 327, 314-326.	2.7	38
175	The Tonian Embu Complex in the Ribeira Belt (Brazil): revision, depositional age and setting in Rodinia and West Gondwana. Precambrian Research, 2019, 320, 31-45.	2.7	38
176	Reconciling Orogenic Drivers for the Evolution of the Bangongâ€Nujiang Tethys During Middle‣ate Jurassic. Tectonics, 2020, 39, e2019TC005951.	2.8	38
177	Acadian basement thrusting, crustal delamination, and structural styles in and around the Humber Arm allochthon, western Newfoundland. Geology, 1988, 16, 370.	4.4	37
178	Thermal evolution of the central Halls Creek Orogen, northern Australia. Australian Journal of Earth Sciences, 1999, 46, 453-465.	1.0	37
179	Crustal growth during island arc accretion and transcurrent deformation, Natal Metamorphic Province, South Africa: New isotopic constraints. Precambrian Research, 2015, 265, 203-217.	2.7	37
180	A paleoproterozoic intra-arc basin associated with a juvenile source in the Southern Brasilia Orogen: Application of U–Pb and Hf–Nd isotopic analyses to provenance studies of complex areas. Precambrian Research, 2016, 276, 178-193.	2.7	37

#	Article	IF	CITATIONS
181	Reconstructing Cryogenian to Ediacaran successions and paleogeography of the South China Block. Precambrian Research, 2018, 314, 452-467.	2.7	37
182	Early Neoproterozoic assembly and subsequent rifting in South China: Revealed from mafic and ultramafic rocks, central Jiangnan Orogen. Precambrian Research, 2019, 331, 105367.	2.7	37
183	Thermochemical lithosphere differentiation and the origin of cratonic mantle. Nature, 2020, 588, 89-94.	27.8	37
184	Provenance of the Earaheedy Basin: implications for assembly of the Western Australian Craton. Precambrian Research, 2004, 128, 343-366.	2.7	36
185	Plume-modified collision orogeny: The Tarim–western Tianshan example in Central Asia. Geology, 2019, 47, 1001-1005.	4.4	35
186	Accretion Tectonics in Western Gondwana Deduced From Smâ€Nd Isotope Mapping of Terranes in the Borborema Province, NE Brazil. Tectonics, 2018, 37, 2727-2743.	2.8	34
187	Early Paleoproterozoic magmatism in the Yangtze Block: Evidence from zircon U-Pb ages, Sr-Nd-Hf isotopes and geochemistry of ca. 2.3†Ga and 2.1†Ga granitic rocks in the Phan Si Pan Complex, north Vietnam. Precambrian Research, 2019, 324, 253-268.	2.7	34
188	Long-lived transcontinental sediment transport pathways of East Gondwana. Geology, 2019, 47, 513-516.	4.4	34
189	Pannotia: in defence of its existence and geodynamic significance. Geological Society Special Publication, 2021, 503, 13-39.	1.3	34
190	Petrogenesis of Archean TTGs and potassic granites in the southern Yangtze Block: Constraints on the early formation of the Yangtze Block. Precambrian Research, 2020, 347, 105848.	2.7	34
191	Mariana-type ophiolites constrain the establishment of modern plate tectonic regime during Gondwana assembly. Nature Communications, 2021, 12, 4189.	12.8	34
192	Early to late Neoproterozoic subduction-accretion episodes in the Cariris Velhos Belt of the Borborema Province, Brazil: Insights from isotope and whole-rock geochemical data of supracrustal and granitic rocks. Journal of South American Earth Sciences, 2019, 96, 102384.	1.4	33
193	Mesoproterozoic rift setting of SW Hainan: Evidence from the gneissic granites and metasedimentary rocks. Precambrian Research, 2019, 325, 69-87.	2.7	33
194	In situ geochemical composition of apatite in granitoids from the eastern Central Asian Orogenic Belt: A window into petrogenesis. Geochimica Et Cosmochimica Acta, 2022, 317, 552-573.	3.9	33
195	Magmatic thickening of crust in non–plate tectonic settings initiated the subaerial rise of Earth's first continents 3.3 to 3.2 billion years ago. Proceedings of the National Academy of Sciences of the United States of America, 2021, 118, .	7.1	33
196	Stratigraphic and structural relations of the southern Dun Mountain Ophiolite Belt and enclosing strata, northwestern Southland, New Zealand. New Zealand Journal of Geology, and Geophysics, 1986, 29, 179-203.	1.8	32
197	Provenance history of the Bangemall Supergroup and implications for the Mesoproterozoic paleogeography of the West Australian Craton. Precambrian Research, 2008, 166, 93-110.	2.7	32
198	Thermal state and evolving geodynamic regimes of the Meso- to Neoarchean North China Craton. Nature Communications, 2021, 12, 3888.	12.8	32

#	Article	IF	CITATIONS
199	A sedimentary archive of tectonic switching from Emeishan Plume to Indosinian orogenic sources in SW China. Journal of the Geological Society, 2014, 171, 269-280.	2.1	31
200	Constraining timing and tectonic implications of Neoproterozoic metamorphic event in the Cathaysia Block, South China. Precambrian Research, 2017, 293, 1-12.	2.7	31
201	Episodic slab rollback and back-arc extension in the Yunnan-Burma region: Insights from Cretaceous Nb-enriched and oceanic-island basalt–like mafic rocks. Bulletin of the Geological Society of America, 2017, 129, 698-714.	3.3	31
202	Convergent continental margin volcanic source for ash beds at the Permian-Triassic boundary, South China: Constraints from trace elements and Hf-isotopes. Palaeogeography, Palaeoclimatology, Palaeoecology, 2019, 519, 154-165.	2.3	31
203	Reconstructing South China in the Mesoproterozoic and its role in the Nuna and Rodinia supercontinents. Precambrian Research, 2020, 337, 105558.	2.7	31
204	Olistoliths and debris flow deposits at ancient consuming plate margins: an eastern Australian example. Sedimentary Geology, 1980, 25, 5-22.	2.1	30
205	Detrital record of mountain building: Provenance of Jurassic foreland basin to the Dabie Mountains. Tectonics, 2010, 29, n/a-n/a.	2.8	30
206	Permo-Triassic detrital records of South China and implications for the Indosinian events in East Asia. Palaeogeography, Palaeoclimatology, Palaeoecology, 2017, 485, 84-100.	2.3	30
207	Characterisation of intraâ€oceanic magmatic arc source terranes by provenance studies of derived sediments. New Zealand Journal of Geology, and Geophysics, 1991, 34, 347-358.	1.8	29
208	Neoarchean magmatic arc in the Western Liaoning Province, northern North China Craton: Geochemical and isotopic constraints from sanukitoids and associated granitoids. Lithos, 2018, 322, 296-311.	1.4	29
209	Provenance history of a Carboniferous Gondwana margin forearc basin, New England Fold Belt, eastern Australia: modal and geochemical constraints. Sedimentary Geology, 1994, 93, 107-133.	2.1	28
210	Shaking a methane fizz: Seismicity from the Araguainha impact event and the Permian–Triassic global carbon isotope record. Palaeogeography, Palaeoclimatology, Palaeoecology, 2013, 387, 66-75.	2.3	28
211	Structural history of ophiolite obduction, Bay of Islands, Newfoundland. Bulletin of the Geological Society of America, 1993, 105, 399-410.	3.3	27
212	Coupled Precambrian crustal evolution and supercontinent cycles: Insights from <i>in-situ</i> U-Pb, O- and Hf-isotopes in detrital zircon, NW india. Numerische Mathematik, 2018, 318, 989-1017.	1.4	27
213	Neoproterozoic I-type and highly fractionated A-type granites in the Yili Block, Central Asian Orogenic Belt: Petrogenesis and tectonic implications. Precambrian Research, 2019, 328, 235-249.	2.7	27
214	Provenance of latest Mesoproterozoic to early Neoproterozoic (meta)-sedimentary rocks and implications for paleographic reconstruction of the Yili Block. Gondwana Research, 2019, 72, 120-138.	6.0	27
215	An Early Cretaceous subduction-modified mantle underneath the ultraslow spreading Gakkel Ridge, Arctic Ocean. Science Advances, 2020, 6, .	10.3	27
216	From Subduction to Collision in the Northern Tibetan Plateau: Evidence from the Early Silurian Clastic Rocks, Northwestern China. Journal of Geology, 2012, 120, 49-67.	1.4	26

#	Article	IF	CITATIONS
217	South China in Rodinia: Constrains from the Neoproterozoic Suixian volcano-sedimentary group of the South Qinling Belt. Precambrian Research, 2018, 314, 170-193.	2.7	26
218	Integrated detrital rutile and zircon provenance reveals multiple sources for Cambrian sandstones in North Gondwana. Earth-Science Reviews, 2021, 213, 103462.	9.1	26
219	Detrital zircon evidence for the reactivation of an Early Paleozoic syn-orogenic basin along the North Gondwana margin in South China. Gondwana Research, 2015, 28, 769-780.	6.0	25
220	Late Permian–Triassic metallogeny in the Chinese Altay Orogen: Constraints from mica 40Ar/39Ar dating on ore deposits. Gondwana Research, 2017, 43, 4-16.	6.0	25
221	Permo–Triassic granitoids, Hainan Island, link to Paleotethyan not Paleopacific tectonics. Bulletin of the Geological Society of America, 2020, 132, 2067-2083.	3.3	25
222	Geochemical character and tectonic significance of Early Devonian keratophyres in the New England Fold Belt, eastern Australia. Australian Journal of Earth Sciences, 1989, 36, 297-311.	1.0	24
223	Provenance of North Atlantic ice-rafted debris during the last deglaciation—A new application of U-Pb rutile and zircon geochronology. Geology, 2013, 41, 155-158.	4.4	24
224	Constructing the Eastern Margin of the Tibetan Plateau During the Late Triassic. Journal of Geophysical Research: Solid Earth, 2018, 123, 10,449.	3.4	24
225	Unravelling depositional setting, age and provenance of the Simlipal volcano-sedimentary complex, Singhbhum craton: Evidence for Hadean crust and Mesoarchean marginal marine sedimentation. Precambrian Research, 2021, 354, 106038.	2.7	24
226	Stratigraphic and structural relations of strata enclosing the Dun Mountain Ophiolite Belt in the Arthurton—Clinton region, Southland, New Zealand. New Zealand Journal of Geology, and Geophysics, 1987, 30, 19-36.	1.8	23
227	The Neoproterozoic southern passive margin of the São Francisco craton: Insights on the pre-amalgamation of West Gondwana from U-Pb and Hf-Nd isotopes. Precambrian Research, 2019, 320, 454-471.	2.7	23
228	The Mesoproterozoic Baoban Complex, South China: A missing fragment of western Laurentian lithosphere. Bulletin of the Geological Society of America, 2020, 132, 1404-1418.	3.3	23
229	Strain localization and fluid-assisted deformation in apatite and its influence on trace elements and U–Pb systematics. Earth and Planetary Science Letters, 2020, 545, 116421.	4.4	23
230	From convergent plate margin to arc–continent collision: Formation of the Kenting Mélange, Southern Taiwan. Gondwana Research, 2016, 38, 171-182.	6.0	22
231	North Atlantic Craton architecture revealed by kimberlite-hosted crustal zircons. Earth and Planetary Science Letters, 2020, 534, 116091.	4.4	22
232	Triassic two-stage intra-continental orogensis of the South China Block, driven by Paleotethyan closure and interactions with adjoining blocks. Journal of Asian Earth Sciences, 2021, 206, 104648.	2.3	22
233	Early Cretaceous subduction in NW Kalimantan: Geochronological and geochemical constraints from the Raya and Mensibau igneous rocks. Gondwana Research, 2022, 101, 243-256.	6.0	22
234	Provenance of late Paleozoic strata in the Yili Basin: Implications for tectonic evolution of the South Tianshan orogenic belt. Bulletin of the Geological Society of America, 2018, 130, 952-974.	3.3	21

#	Article	IF	CITATIONS
235	Neoproterozoic opening of the Pacific Ocean recorded by multi-stage rifting in Tasmania, Australia. Earth-Science Reviews, 2020, 201, 103041.	9.1	21
236	A geochemical study of metabasalts from a subduction complex in eastern Australia. Chemical Geology, 1984, 43, 29-47.	3.3	20
237	Provenance of the Highland Border Complex: constraints on Laurentian margin accretion in the Scottish Caledonides. Journal of the Geological Society, 2012, 169, 575-586.	2.1	20
238	Tectonic settings of continental crust formation: Insights from Pb isotopes in feldspar inclusions in zircon. Geology, 2016, 44, 819-822.	4.4	20
239	Coexisting diverse P–T–t paths during Neoarchean Sagduction: Insights from numerical modeling and applications to the eastern North China Craton. Earth and Planetary Science Letters, 2022, 586, 117529.	4.4	20
240	Frontal vs. basal accretion and contrasting particle paths in metamorphic thrust belts. Geology, 1994, 22, 51.	4.4	19
241	Evolution of the Mozambique Belt in Malawi constrained by granitoid U-Pb, Sm-Nd and Lu-Hf isotopic data. Gondwana Research, 2019, 68, 93-107.	6.0	19
242	Implications of 770â€ <sup>–</sup> Ma Rhyolitic Tuffs, eastern South China Craton in constraining the tectonic setting of the Nanhua Basin. Lithos, 2019, 324-325, 842-858.	1.4	19
243	Hf isotopic ratios in zircon reveal processes of anatexis and pluton construction. Earth and Planetary Science Letters, 2021, 576, 117215.	4.4	19
244	Integrated geochronology and field constraints on subdivision of the Precambrian in China: Data from the Wutaishan. Science Bulletin, 1998, 43, 17-17.	1.7	18
245	Crustal growth and reworking: A case study from the Erguna Massif, eastern Central Asian Orogenic Belt. Scientific Reports, 2019, 9, 17671.	3.3	17
246	Late Paleoproterozoic to Early Mesoproterozoic Mafic Magmatism in the SW Yangtze Block: Mantle Plumes Associated With Nuna Breakup?. Journal of Geophysical Research: Solid Earth, 2020, 125, e2019JB019260.	3.4	17
247	Prototethyan Accretionary Orogenesis Along the East Gondwana Periphery: New Insights From the Early Paleozoic Igneous and Sedimentary Rocks in the Sibumasu. Geochemistry, Geophysics, Geosystems, 2021, 22, e2020GC009622.	2.5	17
248	Resolving the Paleogeographic Puzzle of the Lhasa Terrane in Southern Tibet. Geophysical Research Letters, 2021, 48, e2021GL094236.	4.0	17
249	Evaluating preservation bias in the continental growth record against the monazite archive. Geology, 2022, 50, 243-247.	4.4	17
250	Modal and Geochemical Compositions of the Lower Silurian Clastic Rocks In North Qilian, Nw China: Implications For Provenance, Chemical Weathering, and Tectonic Setting. Journal of Sedimentary Research, 2012, 82, 92-103.	1.6	16
251	Jurassic cooling ages in Paleozoic to early Mesozoic granitoids of northeastern Patagonia: 40Ar/39Ar, 40K–40Ar mica and U–Pb zircon evidence. International Journal of Earth Sciences, 2017, 106, 2343-2357.	1.8	16
252	Detrital record of late-stage silicic volcanism in the Emeishan large igneous province. Gondwana Research, 2020, 79, 197-208.	6.0	16

#	Article	IF	CITATIONS
253	Global-scale emergence of continental crust during the Mesoarchean–early Neoarchean. Geology, 2022, 50, 184-188.	4.4	16
254	From microanalysis to supercontinents: Insights from the Rio Apa Terrane into the Mesoproterozoic SW Amazonian Craton evolution during Rodinia assembly. Journal of Metamorphic Geology, 2022, 40, 631-663.	3.4	16
255	Oxidation of Archean upper mantle caused by crustal recycling. Nature Communications, 2022, 13, .	12.8	16
256	Early tectonic dewatering and brecciation on the overturned sequence at Marble Bar, Pilbara Craton, Western Australia: dome-related or not?. Precambrian Research, 2001, 105, 1-15.	2.7	15
257	Southeastern Lewis Hills (Bay of Islands Ophiolite): Geology of a deeply eroded, inside-corner, ridge-transform intersection. Bulletin of the Geological Society of America, 2001, 113, 1025-1038.	3.3	15
258	Cambrian magmatic flare-up, central Tibet: Magma mixing in proto-Tethyan arc along north Gondwanan margin. Bulletin of the Geological Society of America, 2021, 133, 2171-2188.	3.3	15
259	Evidence for Neoproterozoic terrane accretion in the central Borborema Province, West Gondwana deduced by isotopic and geophysical data compilation. International Geology Review, 2022, 64, 1574-1593.	2.1	15
260	Detrital rutile tracks the first appearance of subduction zone low T/P paired metamorphism in the Palaeoproterozoic. Earth and Planetary Science Letters, 2021, 570, 117069.	4.4	15
261	South Tarim tied to north India on the periphery of Rodinia and Gondwana and implications for the evolution of two supercontinents. Geology, 2022, 50, 131-136.	4.4	15
262	Late cretaceous pelagic sediments, volcanic ASH and biotas from near the Louisville hotspot, Pacific Plate, paleolatitude â^1⁄442°S. Palaeogeography, Palaeoclimatology, Palaeoecology, 1989, 71, 281-299.	2.3	14
263	Nature and record of igneous activity in the Tonga arc, SW Pacific, deduced from the phase chemistry of derived detrital grains. Geological Society Special Publication, 1991, 57, 305-321.	1.3	14
264	Timing and duration of syn-magmatic deformation in the Mabel Downs Tonalite, northern Australia. Journal of Structural Geology, 2000, 22, 1181-1198.	2.3	14
265	Evolving Mantle Sources in Postcollisional Early Permianâ€Triassic Magmatic Rocks in the Heart of Tianshan Orogen (Western China). Geochemistry, Geophysics, Geosystems, 2017, 18, 4110-4122.	2.5	14
266	Metamorphic rocks and plate tectonics. Science Bulletin, 2020, 65, 968-969.	9.0	14
267	Early Paleozoic accretionary orogenesis in the northeastern Indochina and implications for the paleogeography of East Gondwana: constraints from igneous and sedimentary rocks. Lithos, 2021, 382-383, 105921.	1.4	14
268	Anomalous weathering trends indicate accelerated erosion of tropical basaltic landscapes during the Permo-Triassic warming. Earth and Planetary Science Letters, 2022, 577, 117256.	4.4	14
269	Make subductions diverse again. Earth-Science Reviews, 2022, 226, 103966.	9.1	14
270	Dyke domains in the Mitsero graben, Troodos ophiolite, Cyprus: an off-axis model for graben formation at a spreading centre. Journal of the Geological Society, 1995, 152, 923-932.	2.1	13

#	Article	IF	CITATIONS
271	Geology, geochronology and isotopic geochemistry of the Xiaoliugou W–Mo ore field in the Qilian Orogen, NW China: Case study of a skarn system formed during continental collision. Ore Geology Reviews, 2017, 81, 575-586.	2.7	13
272	A long-lived active margin revealed by zircon U–Pb–Hf data from the Rio Apa Terrane (Brazil): New insights into the Paleoproterozoic evolution of the Amazonian Craton. Precambrian Research, 2020, 350, 105919.	2.7	13
273	Recognition of the Phanerozoic "Young granite gneiss―in the central Yeongnam massif. Geosciences Journal, 2015, 19, 1-16.	1.2	12
274	Differentiating continental and oceanic arc systems and retro-arc basins in the Jiangnan orogenic belt, South China. Geological Magazine, 2019, 156, 2001-2016.	1.5	12
275	Linking South China to North India from the late Tonian to Ediacaran: Constraints from the Cathaysia Block. Precambrian Research, 2020, 350, 105898.	2.7	12
276	Denuding a Craton: Thermochronology Record of Phanerozoic Unroofing From the Pilbara Craton, Australia. Tectonics, 2020, 39, e2019TC005988.	2.8	12
277	Southern extension of the Paleotethyan zone in SE Asia: Evidence from the Permo-Triassic granitoids in Malaysia and West Indonesia. Lithos, 2021, 398-399, 106336.	1.4	12
278	Aulacogen Formation in Response to Opening the Ailaoshan Ocean: Origin of the Qin-Fang Trough, South China. Journal of Geology, 2017, 125, 531-550.	1.4	12
279	Zircon U-Pb age, trace element, and Hf isotopic constrains on the origin and evolution of the Emeishan Large Igneous Province. Gondwana Research, 2022, 105, 535-550.	6.0	12
280	Jurassic subduction of the Paleo-Pacific plate in Southeast Asia: New insights from the igneous and sedimentary rocks in West Borneo. Journal of Asian Earth Sciences, 2022, 232, 105111.	2.3	12
281	Provenance mixing in an intraoceanic subduction zone: Tonga Trench-Louisville Ridge collision zone, southwest Pacific. Sedimentary Geology, 1990, 67, 35-53.	2.1	11
282	Provenance Record of Late Mesoproterozoic to Early Neoproterozoic Units, West Hainan, South China, and Implications for Rodinia Reconstruction. Tectonics, 2020, 39, e2020TC006071.	2.8	11
283	Crust-mantle geodynamic origin of ~2.7ÂGa granitoid diversification in the Jiaobei terrane, North China Craton. Precambrian Research, 2020, 346, 105821.	2.7	11
284	Petrochronological constraints and tectonic implications of Tonian metamorphism in the Embu Complex, Ribeira Belt, Brazil. Precambrian Research, 2021, 363, 106315.	2.7	11
285	Characteristics of Hg concentrations and isotopes in terrestrial and marine facies across the end-Permian mass extinction. Global and Planetary Change, 2021, 205, 103592.	3.5	11
286	Temporal and Spatial Variations of Enriched Source Components in Linzizong Volcanic Succession, Tibet, and Implications for the India–Asia Collision. Journal of Petrology, 2022, 63, .	2.8	11
287	Origin of culminations within the Southeast Oman Mountains at Jebel Ma-jhool and Ibra Dome. Geological Society Special Publication, 1990, 49, 429-445.	1.3	10
288	Base-up growth of ocean crust by multiple phases of magmatism: field evidence from Macquarie Island. Journal of the Geological Society, 2004, 161, 739-742.	2.1	10

#	Article	IF	CITATIONS
289	Geochemistry, 40Ar/39Ar geochronology, and geodynamic implications of Early Cretaceous basalts from the western Qinling orogenic belt, China. Journal of Asian Earth Sciences, 2018, 151, 62-72.	2.3	10
290	Diversity of late Neoarchean K-rich granitoid rocks derived from subduction-related crust/mantle interactions in the Jiaobei terrane, North China Craton. Gondwana Research, 2020, 85, 84-102.	6.0	10
291	The chondritic neodymium stable isotope composition of the Earth inferred from mid-ocean ridge, ocean island and arc basalts. Geochimica Et Cosmochimica Acta, 2021, 293, 575-597.	3.9	10
292	Middle Neoproterozoic (ca. 700ÂMa) tectonothermal events in the Lhasa terrane, Tibet: Implications for paleogeography. Gondwana Research, 2022, 104, 252-264.	6.0	10
293	Using zircon in mafic migmatites to disentangle complex high-grade gneiss terrains – Terrane spotting in the Lewisian complex, NW Scotland. Precambrian Research, 2021, 355, 106074.	2.7	10
294	Evaluating sediment recycling through combining inherited petrogenic and acquired sedimentary features of multiple detrital minerals. Basin Research, 2022, 34, 1055-1083.	2.7	10
295	Structural history of the metamorphic sole of the Bay of Islands Complex, western Newfoundland. Canadian Journal of Earth Sciences, 1995, 32, 533-544.	1.3	9
296	Multistage deformation of linked fault systems in extensional regions: An example from the northern Perth Basin, Western Australia. Australian Journal of Earth Sciences, 1999, 46, 897-903.	1.0	9
297	Large-Scale Translation of Accreted Terranes Along Continental Margins. Gondwana Research, 2001, 4, 628-629.	6.0	9
298	A non-zircon Hf isotope record in Archean black shales from the Pilbara craton confirms changing crustal dynamics ca. 3 Ga ago. Scientific Reports, 2018, 8, 922.	3.3	9
299	The Missing Magmatic Arc in a Longâ€Lived Ocean From the Western Kunlun―Pamir Paleoâ€Tethys Realm. Geophysical Research Letters, 2021, 48, .	4.0	9
300	Cretaceous Tethyan subduction in SE Borneo: Geochronological and geochemical constraints from the igneous rocks in the Meratus Complex. Journal of Asian Earth Sciences, 2022, 226, 105084.	2.3	9
301	Acadian orogeny in west Newfoundland: Definition, character, and significance. Special Paper of the Geological Society of America, 1993, , 135-152.	0.5	8
302	Crustal reworking at convergent margins traced by Fe isotopes in I-type intrusions from the Gangdese arc, Tibetan Plateau. Chemical Geology, 2019, 510, 47-55.	3.3	8
303	Petrogenesis and tectonic implications of Early Cretaceous andesitic–dacitic rocks, western Qinling (Central China): Geochronological and geochemical constraints. Geoscience Frontiers, 2019, 10, 1507-1520.	8.4	8
304	Cretaceous Kuching accretionary orogenesis in Malaysia Sarawak: Geochronological and geochemical constraints from mafic and sedimentary rocks. Lithos, 2021, 400-401, 106425.	1.4	8
305	Processes of Ophiolite Emplacement in Oman and Newfoundland. Petrology and Structural Geology, 1991, , 501-516.	0.5	8
306	Re-initiation of plutonism at the Gondwana margin after a magmatic hiatus: The bimodal Permian-Triassic Longwood Suite, New Zealand. Gondwana Research, 2022, 105, 432-449.	6.0	8

#	Article	IF	CITATIONS
307	Transfer zones normal and oblique to rift trend: examples from the Perth Basin, Western Australia. Geological Society Special Publication, 2001, 187, 475-488.	1.3	7
308	Craton to Regional-scale analysis of the Birimian of West Africa. Precambrian Research, 2016, 274, 1-2.	2.7	7
309	Survival of the Lhasa Terrane during its collision with Asia due to crust-mantle coupling revealed by ca. 114†Ma intrusive rocks in western Tibet. Lithos, 2018, 304-307, 200-210.	1.4	7
310	Using apatite to resolve the age and protoliths of mid-crustal shear zones: A case study from the Taxaquara Shear Zone, SE Brazil. Lithos, 2020, 378-379, 105817.	1.4	7
311	Implications for supercontinent reconstructions of mid-late Neoproterozoic volcanic – Sedimentary rocks from the Cathaysia Block, South China. Precambrian Research, 2021, 354, 106056.	2.7	7
312	Archean trondhjemitic crust at depth in Yangtze Craton: Evidence from TTG xenolith in mafic dyke and apatite inclusion pressure in zircon. Precambrian Research, 2021, 354, 106055.	2.7	7
313	Forging isotopically juvenile metamorphic zircon from and within Archean TTG gneiss: Whole-rock Sr-Nd-Pb and zircon U-Pb-Hf-REE constraints. Chemical Geology, 2022, 590, 120710.	3.3	7
314	Acadian remobilization of a Taconian ophiolite, Hare Bay allochthon, northwestern Newfoundland. Geology, 1989, 17, 257.	4.4	6
315	Quantifying temperature variation between Neoproterozoic cryochron – nonglacial interlude, Nanhua Basin, South China. Precambrian Research, 2020, 351, 105967.	2.7	6
316	Isotopic and geochemical constraints for a Paleoproterozoic accretionary orogen in the Borborema Province, NE Brazil: Implications for reconstructing Nuna/Columbia. Geoscience Frontiers, 2021, , 101167.	8.4	6
317	Strain Partitioning along Terrane Bounding and Intraterrane Shear Zones: Constraints from a Long-Lived Transpressional System in West Gondwana (Ribeira Belt, Brazil). Lithosphere, 2022, 2021, .	1.4	6
318	Craton Formation in Early Earth Mantle Convection Regimes. Journal of Geophysical Research: Solid Earth, 2022, 127, .	3.4	6
319	Early Cretaceous subduction-modified lithosphere beneath the eastern Qinling Orogen revealed from the Daying volcanic sequence in central China. Journal of Asian Earth Sciences, 2019, 176, 209-228.	2.3	5
320	Synchronous late Neoarchean Na- and K-rich granitoid magmatism at an active continental margin in the Eastern Liaoning Province of North China Craton. Lithos, 2020, 376-377, 105770.	1.4	5
321	Setting and formation of the earliest Neoproterozoic rifted arc Pingshui VMS deposit, South China. Precambrian Research, 2022, 369, 106548.	2.7	5
322	Polymetamorphism of mafic granulites in the North China Craton: textural and thermobarometric evidence and tectonic implications. Geological Society Special Publication, 2001, 184, 323-341.	1.3	4
323	Generation of syn-collisional S-type granites in collision zones: An example from the Late Triassic Tanggula Batholith in northern Tibet. Gondwana Research, 2022, 104, 185-198.	6.0	4
324	Testing the advantages of simultaneous in-situ Sm Nd, U Pb and elemental analysis of igneous monazite for petrochronological studies. An example from the late Archean, Penzance granite, Western Australia. Chemical Geology, 2022, 594, 120760.	3.3	4

#	Article	IF	CITATIONS
325	Deformation, thermochronology and tectonic significance of the crustal-scale Cubatão Shear Zone, Ribeira Belt, Brazil. Tectonophysics, 2022, 828, 229278.	2.2	4
326	Leucogranite Records Multiple Collisional Orogenies. Geophysical Research Letters, 2022, 49, .	4.0	4
327	Tectonic insights of the southwest Amazon Craton from geophysical, geochemical and mineralogical data of Figueira Branca mafic-ultramafic suite, Brazil. Tectonophysics, 2017, 708, 96-107.	2.2	3
328	Geochronological and geochemical constraints on the subduction-modified lithospheric origin of the early Cretaceous volcanic rocks, in the western North Huaiyang Belt of Dabie Orogen, China. Journal of the Geological Society, 2020, 177, 170-188.	2.1	3
329	Was there an exchange of detritus between the northern and southern Black Sea terranes in the Mesozoic-early Cenozoic?. Gondwana Research, 2021, , .	6.0	3
330	Calibrating the Yield Strength of Archean Lithosphere Based on the Volume of Tonalite-Trondhjemite-Granodiorite Crust. Frontiers in Earth Science, 0, 8, .	1.8	3
331	Comment and Reply on "Structure of the Appalachian deformation front in western Newfoundland: Implications of multichannel seismic reflection data". Geology, 1991, 19, 951.	4.4	2
332	Cenozoic retrogression and exhumation of the amphibolites in the eastern Gangdese Belt, SW China. Journal of Asian Earth Sciences, 2021, 205, 104574.	2.3	2
333	An Early Garnet Redoxâ€Filter as an Additive Oxidizer in Lower Continental Arc Crust Traced Through Fe Isotopes. Journal of Geophysical Research: Solid Earth, 2021, 126, e2020JB021217.	3.4	2
334	A Forearc Stratigraphic Response to Cretaceous Plateau Collision and Slab Detachment, South Island, New Zealand. Tectonics, 2021, 40, e2021TC006806.	2.8	2
335	Untangling the history of oroclines and mountain belts. National Science Review, 2022, 9, nwab211.	9.5	2
336	Ordovician amphibolite-facies metamorphism in Hainan Island: A record of early Paleozoic accretionary orogenesis along the northern margin of East Gondwana?. Journal of Asian Earth Sciences, 2022, 229, 105161.	2.3	2
337	Mercury anomalies across the Cryogenian-Ediacaran boundary in South China. Precambrian Research, 2022, 379, 106771.	2.7	2
338	Understanding earthquakes using the geological record: an introduction. Philosophical Transactions Series A, Mathematical, Physical, and Engineering Sciences, 2021, 379, 20190410.	3.4	1
339	Marine productivity variations and environmental perturbations across the early Triassic Smithian-Spathian boundary: Insights from zinc and carbon isotopes. Global and Planetary Change, 2021, 205, 103579.	3.5	1
340	Late Neoproterozoic palaeogeography: the Laurentia-Baltica puzzle. Journal of the Virtual Explorer, 0, 22, .	0.0	1
341	Subduction-related mantle metasomatism and partial melting in the northern North China Craton: Insights from amphibolite enclaves, Siziwangqi, Inner Mongolia. Precambrian Research, 2021, 355, 106002.	2.7	0
342	Key Role for Geoscientists in Providing ?Early Warning System? on Environmental Crises. Pacific Conservation Biology, 2008, 14, 231.	1.0	0

#	Article	IF	CITATIONS
343	SHORT EPISODES OF CRUST GENERATION DURING PROTRACTED ACCRETIONARY PROCESSES: EVIDENCE FROM CENTRAL ASIAN OROGENIC BELT, NW CHINA. Geodinamika I Tektonofizika, 2017, 8, 573-574.	0.7	Ο
344	Report on the Ad-hoc Review of the IUGS Commission on Tectonics and Structural Geology (TecTask). Episodes, 2019, 42, 355-358.	1.2	0
345	Lithosphere beneath the Evolving Tianshan Orogen: Constraints from Xenoliths. Lithosphere, 2022, 2022, .	1.4	0